



Effects of photobiomodulation on different application points and different phases of complex regional pain syndrome type I in the experimental model

Jaqueline Betta Canever¹, Rafael Inácio Barbosa^{1,2}, Ketlyn Germann Hendler^{1,2},
Lais Mara Siqueira das Neves^{1,3}, Heloyse Uliam Kuriki^{1,2}, Aderbal Silva Aguiar Júnior²,
Marisa de Cassia Registro Fonseca³, and Alexandre Márcio Marcolino^{1,2}

¹Laboratory of Assessment and Rehabilitation of the Locomotor Apparatus, Department of Health Sciences, Center Araranguá, Federal University of Santa Catarina, Araranguá, Brazil

²Postgraduate Program in Rehabilitation Sciences, Federal University of Santa Catarina, Araranguá, Brazil

³Postgraduate Program in Rehabilitation and Functional Performance of the Department of Health Sciences, Ribeirão Preto School of Medicine, University of São Paulo, Ribeirão Preto, Brazil

Received January 19, 2021

Revised April 17, 2021

Accepted April 17, 2021

Handling Editor: Sang Hun Kim

Correspondence

Alexandre Márcio Marcolino
Department of Health Sciences, Federal
University of Santa Catarina, Campus
Jardim das Avenidas, Rod. Gov. Jorge
Lacerda, 3201, Araranguá 88906-072,
Brazil
Tel: +55-48-98820-0693
Fax: +55-48-3522-2408
E-mail: alexandre.marcolino@ufsc.br

Background: Complex regional pain syndrome type I (CRPS-I) consists of disorders caused by spontaneous pain or induced by some stimulus. The objective was to verify the effects of photobiomodulation (PBM) using 830 nm wavelength light at the affected paw and involved spinal cord segments during the warm or acute phase.

Methods: Fifty-six mice were randomized into seven groups. Group (G) 1 was the placebo group; G2 and G3 were treated with PBM on the paw in the warm and acute phase, respectively; G4 and G5 treated with PBM on involved spinal cord segments in the warm and acute phase, respectively; G6 and G7 treated with PBM on paw and involved spinal cord segments in the warm and acute phase, respectively. Edema degree, thermal and mechanical hyperalgesia, skin temperature, and functional quality of gait (Sciatic Static Index [SSI] and Sciatic Functional Index [SFI]) were evaluated.

Results: Edema was lower in G3 and G7, and these were the only groups to return to baseline values at the end of treatment. For thermal hyperalgesia only G3 and G5 returned to baseline values. Regarding mechanical hyperalgesia, the groups did not show significant differences. Thermography showed increased temperature in all groups on the seventh day. In SSI and SFI assessment, G3 and G7 showed lower values when compared to G1, respectively.

Conclusions: PBM irradiation in the acute phase and in the affected paw showed better results in reducing edema, thermal and mechanical hyperalgesia, and in improving gait quality, demonstrating efficacy in treatment of CRPS-I symptoms.

Key Words: Complex Regional Pain Syndromes; Edema; Hyperalgesia; Laser Therapy; Mice; Models, Animal; Pain; Pain Management; Reflex Sympathetic Dystrophy; Skin Temperature; Temperature; Thermography.

© This is an open-access article distributed under the terms of the Creative Commons Attribution Non-Commercial License (<http://creativecommons.org/licenses/by-nc/4.0/>), which permits unrestricted non-commercial use, distribution, and reproduction in any medium, provided the original work is properly cited.

© The Korean Pain Society, 2021

Author contributions: Jaqueline Betta Canever: Writing/manuscript preparation; Rafael Inácio Barbosa: Methodology; Ketlyn Germann Hendler: Investigation; Lais Mara Siqueira das Neves: Computation; Heloyse Uliam Kuriki: Study conception; Aderbal Silva Aguiar Júnior: Resources; Marisa de Cassia Registro Fonseca: Investigation; Alexandre Márcio Marcolino: Writing/manuscript preparation.

INTRODUCTION

Complex regional pain syndrome (CRPS), which consists of disorders caused by spontaneous pain or pain that is induced by some stimulus, is accompanied by a wide variety of autonomic and motor disorders [1,2]. Pain is the main symptom after trauma and may be associated with changes in skin color, limb temperature, motor activity or also edema [3]. There are two types of CRPS: type I and type II [4].

Complex regional pain syndrome type I (CRPS-I) appears after a harmful stimulus, without nerve damage [2]. In most cases CRPS has three stages [5]. The first stage is called the “warm phase”, in which the patient’s limb feels sore and swollen, accompanied by a neurogenic inflammation [6]. In the second stage, or acute phase, there is an activation of keratinocytes, proliferation and expression of inflammatory mediators as a tumor necrosis factor alpha (TNF α), interleukin (IL)-1 β and IL-6, nerve growth factor, and activation of mast cells [2,6]. In the third stage, or chronic phase, the limb becomes cold, dystrophic, even more painful, and hypersensitive [1].

The acute phase of CRPS-I can often be treated with early physiotherapy only. However, the chronic phase rarely resolves spontaneously, causing permanent discomfort in patients [2]. The consequences include changes in the sensory, motor, and autonomic nervous systems to cognitive deficits and vascular dysfunctions [7,8]. However, there is still no gold standard for CRPS-I treatment [6]. Although physiotherapy or occupational therapy is indicated as a first-line treatment [6,8], other interventions are also prescribed, such as psychological therapy, drug management, surgical intervention [9,10], and even amputation [11,12].

Along the spectrum of physiotherapy, some studies have suggested the use of electrophysical agents for the complementary treatment of CRPS-I, such as photobiomodulation (PBM) [12-14]. PBM seems to enhance the effects of sodium-potassium pumps. This reverses the inhibition of mitochondria, stimulates cell proliferation, and increases the metabolism [15,16]. The absorption of infrared photons by mitochondrial cytochrome C oxidase leads to an increase in adenosine triphosphate (ATP), nitric oxide, and reactive oxygen, improving cellular energy supply and stimulating signal transduction, which inhibits peripheral sensitization, leading to reductions in inflammatory neuropeptides and increased release of serotonin and endorphin [16].

In the peripheral nervous system, PBM acts by reducing pain through increased activity of acetylcholinesterase in the synapses, synthesis of serotonin and endorphin, temporary suppression of action potentials, and inhibition of the sodium-potassium-ATPase pump [17]. However, few studies explain the direct effects of PBM on CRPS-I trans-

mission. This study examined the effects of PBM using 830 nm wavelength light at the affected paw and involved spinal cord segments (lumbar 4 and 5) and during the warm or acute phase of the disease.

MATERIALS AND METHODS

1. Ethical consideration

All protocols and procedures used in this study were approved by the Animal Experimentation Ethics Committee of the Federal University of Santa Catarina (UFSC) under number 1474140817. This study is based on the 3 Rs principle (replacement, reduction, and refinement). The manuscript was written according to the ARRIVE (Animal Research: Reporting of *In Vivo* Experiments) checklist.

2. Experimental procedure

In this study, 56 Swiss mice (40-65 g) were used, which were moved from the Central Bioterium of the UFSC and maintained in the bioterium sector of Campus Araranguá - UFSC. The animals were kept in isolated cages with constant temperature (22°C \pm 2°C) and humidity (60%-80%) in a 12-hour light-dark cycle with free access to water and feed throughout the experimental period. The experiment had a duration of twenty-one days and five evaluations were performed. Before the induction (basal), after 3 days, the 7th day, 14th day, and 21st day. At the end of the experiment the animals were euthanized orally with excess ketamine hydrochloride (Agener União[®], São Paulo, Brazil) associated with xylazine hydrochloride Dopaser[®] (Paulínia, Brazil).

To induce CRPS-I, the chronic post-ischemia pain (CPIP) model was used [17,18]. For this, the animals were anesthetized with an intraperitoneal injection of ketamine hydrochloride (Agener União[®]) 100 mg/kg associated with xylazine hydrochloride Dopaser[®] 10 mg/kg (manual of standards of the Laboratory of Operative Technique and Experimental Surgery - UFSC, 2013). The procedure lasted three hours (09:00 to 12:00). After anesthesia, an elastic ring with an internal diameter of 1.3 mm (elastic band 60.03.302; Morelli, São Paulo, Brazil) was placed in an area proximal to the ankle joint of the right hind leg (Fig. 1) where it remained for 3 hours in order to make a tourniquet and induce ischemia [19]. In the third hour, the elastic ring was cut and reperfusion occurred (Fig. 1). To evaluate if the CPIP was successful, mechanical allodynia needed to be found in the right and left limbs, and the experimental limb needed to have a 30% reduction in the mechanical threshold within 48 hours after induction [20]. The

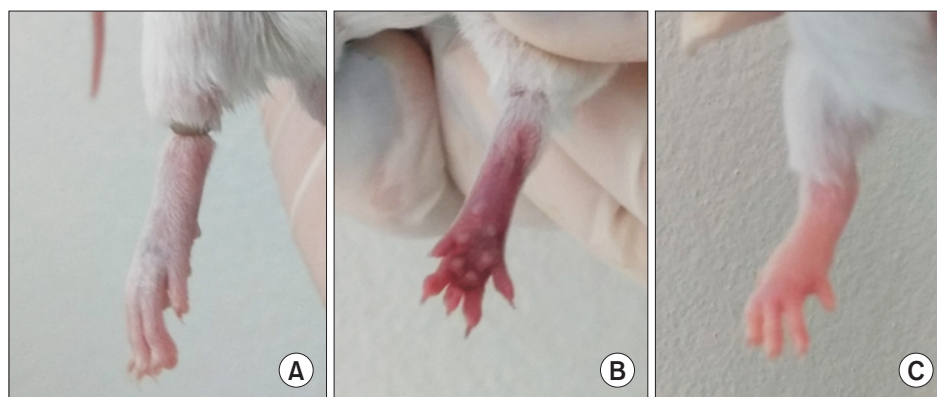


Fig. 1. Representative photographs during tourniquet exposure (A), 2 after reperfusion (B) and 1 hour after tourniquet removal (C). Note in the second image the tissue hypoxia and in the third image, after tourniquet removal, hyperemia with apparent edema.

warm phase was considered after 1 day of the CPIP [5]. The groups were considered to be in the acute phase of CRPS-I on day 3 after CPIP. There is no consensus about when CRPS-I becomes acute; in the literature there are studies that consider it acute after 1 day of CPIP [1] and others after 3 weeks of CPIP [21]. In the present study we considered the acute phase to be from day 3, since the mice presented inflammation, hyperalgesia, and allodynia. The chronic phase will not be addressed due to the onset being 7 weeks after CPIP [21].

All 56 mice were randomized into seven experimental groups, each group with 8 animals. The groups were divided as follows.

- Group 1 - control or placebo, the PBM was not applied;
- Group 2 - PBM applied to the paw with CRPS-I from the warm phase (1st day after CPIP induction);
- Group 3 - PBM applied to the paw from the acute phase of CRPS-I (3rd day after CPIP induction);
- Group 4 - PBM applied near the region between the L4 and L5 segments from the warm phase of the injury;
- Group 5 - PBM applied near the region between the L4 and L5 segments from the acute phase of the lesion;
- Group 6 - PBM applied at two points: the right paw and the region between the L4 and L5 segments from the warm phase of the syndrome;
- Group 7 - PBM applied at two points: the right paw and the region between the L4 and L5 segments from the acute phase of the injury.

3. PBM

The aluminum laser diode and gallium arsenide with a wavelength of 830 nm, continuous beam, from Ibramed[®] Equipamentos Médicos, São Paulo, Brazil was used. The parameters related to PBM are listed in Table 1. The PBM was applied with the contact point mode in all groups, the

Table 1. Parameters of photobiomodulation

Variable	Parameter
Photobiomodulator	Infrared laser
Wavelength (nm)	830
Frequency (Hz)	Continuous
Power (mW)	30
Output beam (cm ²)	0.11
Power density (mW/cm ²) - each	19.44
Application point	1
Dose (J/cm ²)	10
Time (sec)	40
Energy by point (J)	1.2

application site was on the paw and region between the L4 and L5 segments. The lumbar segment 3 and predominantly the L4 and L5 are associated with the sciatic nerve [22], so they were selected as the PBM application site. The study by Chen et al. [23] demonstrated that in the CPIP model, the dorsal horn of the spinal cord plays a critical role in the integration of pain signals and sensitization. In the CPIP model in mongooses, in the dorsal horn of the spinal cord, non-neuronal cells such as astrocytes and microglia are activated in order to produce pro-inflammatory mediators to modulate the pain process. In addition, CRPS-I shows increased expression of genes (substance P and calcitonin genes), especially at the ipsilateral levels of L4 and L5 [22]. Therefore, it was thought interesting to see if the segments between L4 and L5 are therapeutic targets for the treatment of CRPS-I in mice.

Some studies demonstrate that the best penetration wavelengths are between 760 and 830 nm [24-26], the penetration of 830 nm PBM in mouse skin, for example, is approximately 40% to 42% [24]. It should be noted that the transmitting power of PBM in skin, fat, and muscle decreases with increasing thickness [24]. In addition, the wavelength, at about 808 nm, penetrates the scalp, skull, meninges, and brain of humans to approximately 40 mi-

limeters [27]. Hamblin et al. [27] described a penetration with wavelengths near infrared can arrive the 50 millimeters. For the application in the medullary region and in the peripheral nervous tissue region we used, in this research, PBM with a wavelength of 830 nm. To determine the site of application of PBM, the spine region of the mice was palpated and the region between thoracic vertebrae 11 and 12 was marked with a pen [28]. The demarcation with the pen was performed in such a way that PBM could always be applied in the same place, thus avoiding the risk of bias.

4. Analysis procedure

1) Edema

A digital micrometer (Digimess, São Paulo, Brazil) was used to measure the paw edema with CRPS-I. The instrument was calibrated, with a capacity of 0-25 mm and precision of 0.001 mm. Three repeated compressions were performed. The data were expressed in millimeters [12,20].

2) Thermal hyperalgesia

The evaluation of thermal hyperalgesia was performed as described by Hargreaves et al. [29]. For this, the Hargreaves device (Ugo Basile, Gemonio, Italy) was used, which emitted an infrared light source which directly irradiated the affected paw of the mouse. The withdrawal latency was measured through an automatic sensor. The time of 22 seconds was determined as the cut-off in order to avoid possible tissue damage to the animals' paws. Three response time measurements were performed at 20 minutes intervals. The animals were evaluated before the induction procedure, and on the 3rd, 7th, 14th, and 21st day after the injury.

3) Mechanical hyperalgesia

The evaluation procedure of mechanical hyperalgesia was performed using the Von Frey manual test (Stoelting, Chicago, IL). This test was developed by Maximilian Von Frey, and evaluates mechanical allodynia in rodents. It is considered gold standard in the determination of mechanical thresholds [22,23]. For the test, the animals were individually allocated in acrylic boxes (9 × 7 × 11 cm) on raised wire platforms, which allow access to the plantar surface of the animals' rear right paw. The frequency of withdrawal response was evaluated after 10 applications, with an interval of 1 second. The filament (0.4 g) was configured from previous studies to produce an average withdrawal frequency of about 15%, suitable for measuring mechanical hyperalgesia [30,31].

4) Thermographic analysis

The FLIR C2 chamber (FLIR® Systems Inc., Wilsonville, OR) with a spectral range of 7.5-14 μm, spatial resolution (instantaneous field of view) of 11 mrad, and sensitivity of 100 mK was used to assess skin temperature. The camera is equipped with an uncooled microbolometer with a detector field of 17 μm, a temperature range of -10°C to + 150°C, accuracy of ± 2°C or 2% to 25°C, 9 Hz image frequency, and a 320 × 240 pixels display. Emissivity was adjusted to 0.95, reflected temperature 30°C. The photos were analyzed using FLIR Tools software (FLIR® Systems Inc.), with the temperature scale maintained from 20 to 40°C.

5) Functional and Sciatic Static Index (SSI)

A non-invasive way to evaluate the functioning of the sciatic nerve is through walking [24,25,32,33]. For this, the Sciatic Functional Index (SFI) was introduced by de Medinaceli et al. [34]. This method aims to analyze the degree of sciatic nerve injury and recovery, and its results range from 0 to -100, in which 0 is the absence of nerve injury and -100 means complete dysfunction. This method uses as parameters the footprint length, finger extension, and intermediate finger extension (Fig. 2). To assess the SFI, a 43 cm long, 5.5 cm high, and 8.7 cm wide transparent acrylic walkway with was used, with a wooden casing at the end. An 8 megapixel camera (Sony™, Tokyo, Japan) was positioned just below the catwalk and captured the videos of the animals walking. To analyze the images, the software Kinovea™ (Boston, MA) Footprint Imaging and Image J™ (Boston, MA) were used. The SFI values were found through the formula proposed by Bain et al. [35].

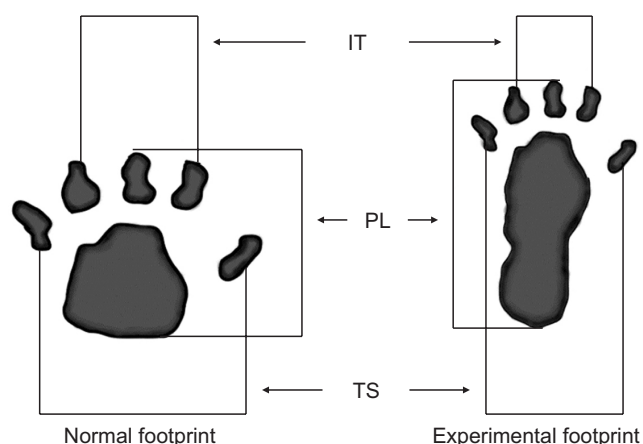


Fig. 2. Illustrative representation of the parameters used to calculate the Sciatic Static Index and Sciatic Functional Index. IT: intermediate finger opening, PL: footprint length, TS: full finger opening. Adapted from the article of Marcolino et al. (*J Hand Microsurg* 2013; 5: 49-53) [33].

According studies [28,29,36,37], the SSI has been shown to be effective in evaluating gait, possibly more accurate than the SFI. To evaluate the SSI, the same acrylic walkway and camera were used. The images were scanned and evaluated by Image J™ software, to transform pixels into millimeters and calculate the parameters (Fig. 2). The evaluations referring to the SFI and SSI were made at four points: the 3rd, 7th, 14th, and 21st day. In all, 448 images were analyzed, 224 for the SSI and 224 for the SFI. It is also described that, because CRPS-I presents with mild and subtle injury to the sciatic nerve, it goes unnoticed in most cases [38]. Furthermore, in previous studies [13], a change

in the support of the affected paw of the mice was verified, which allowed us to evaluate using the SFI and the SSI.

5. Statistical analysis

The normality of the data was tested using the Shapiro-Wilk test. The two-way analysis of variance (ANOVA) and the Bonferroni post-hoc test were used to analyze the statistical differences between the groups in each variable. SPSS Statistics 23.0 (IBM Co., Armonk, NY) and GraphPad Prism® 8.0 (GraphPad Software, San Diego, CA) software were used for the analysis. The significance level used was $P < 0.05$. The results were expressed as mean ± standard error of the mean.

RESULTS

1. Edema

The mean values and standard deviation of the edema variable are shown in Fig. 3 and Table 2. Statistically significant differences were observed only between G1 vs. G6 ($P < 0.015$) on the 3rd day. On the 7th day, significant differences were found between G1 vs. G2 ($P < 0.031$); G2 vs. G5 ($P < 0.005$) and G6 ($P < 0.001$), as well as G3 vs. G5 ($P < 0.001$) and G6 ($P < 0.027$).

On the 14th day, statistically significant differences were found between G5 vs. G1 ($P < 0.009$), G2 ($P < 0.005$), G3 ($P < 0.005$), G4 ($P < 0.002$), G6 ($P < 0.001$) and G7 ($P < 0.049$). On the 21st day, significant differences were found between G3 vs. G2 ($P < 0.009$), G5 ($P < 0.005$), G6 ($P < 0.005$); G4 vs. G5 ($P < 0.001$), G6 ($P < 0.002$) as well as G7 vs. G2 ($P < 0.023$), G6 ($P < 0.005$). On the last day of the evaluation, only G3 and G7 returned to their basal paw diameter levels, demonstrating effectiveness in treatment. G1, G2, G5, and G6 presented higher values of affected limb diameter, which

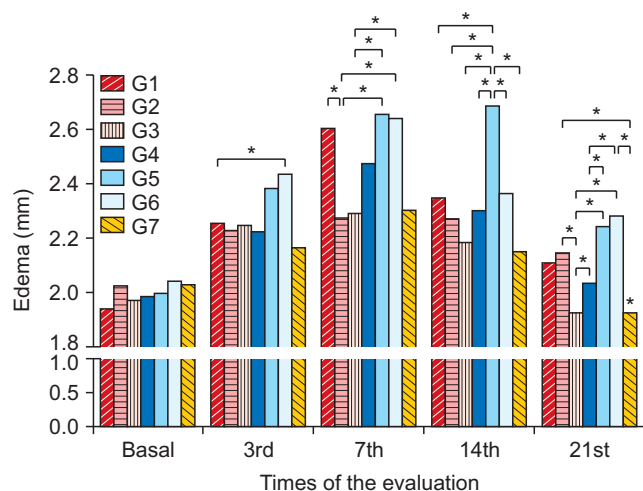


Fig. 3. Average values of the edema variable between groups and evaluation days. Group (G) 1: control (placebo), G2: photobiomodulation (PBM) applied to the paw with complex regional pain syndrome type I (CRPS-I) from the warm phase, G3: PBM applied to the paw with CRPS-I from the acute phase, G4: PBM applied close to the area of the region between L4 and L5 from the warm phase, G5: PBM applied close to the area of the region between L4 and L5 from the acute phase, G6: PBM applied at two points: right paw and region between L4 and L5 from the warm phase, G7: PBM applied at two points: right paw and region between L4 and L5 from the acute phase. * $P < 0.05$.

Table 2. Mean and standard deviation values for paw edema according to groups and evaluations

Paw edema	Group						
	1	2	3	4	5	6	7
Basal	1.94 ± 0.07	2.03 ± 0.04	1.97 ± 0.13	1.99 ± 0.08	2.00 ± 0.06	2.04 ± 0.11	2.03 ± 0.05
3rd	2.26 ± 0.27	2.23 ± 0.11	2.25 ± 0.17	2.23 ± 0.06	2.39 ± 0.16	2.44 ± 0.16	2.17 ± 0.13
7th	2.60 ± 0.18	2.28 ± 0.19	2.29 ± 0.30	2.48 ± 0.31	2.66 ± 0.32	2.64 ± 0.18	2.30 ± 0.35
14th	2.35 ± 0.20	2.27 ± 0.13	2.19 ± 0.37	2.30 ± 0.16	2.69 ± 0.33	2.37 ± 0.28	2.15 ± 0.19
21st	2.11 ± 0.06	2.15 ± 0.08	1.93 ± 0.04	2.03 ± 0.07	2.24 ± 0.28	2.28 ± 0.29	1.93 ± 0.05

Group 1: control (placebo), Group 2: photobiomodulation (PBM) applied to the paw with complex regional pain syndrome type I (CRPS-I) from the warm phase, Group 3: PBM applied to the paw with CRPS-I from the acute phase, Group 4: PBM applied close to the area of the region between L4 and L5 from the warm phase, Group 5: PBM applied close to the area of the region between L4 and L5 from the acute phase, Group 6: PBM applied at two points: right paw and region between L4 and L5 from the warm phase, Group 7: PBM applied at two points: right paw and region between L4 and L5 from the acute phase, 3rd: third evaluation day, 7th: seventh evaluation day, 14th: fourteenth evaluation day, 21st: twenty-first evaluation day.

demonstrates that the treatment in these groups was not effective in controlling edema.

2. Thermal hyperalgesia

The average values referring to the evaluation of thermal hyperalgesia through the Hargreaves test are shown in Fig. 4 and Table 3. On the 3rd day there were no statistical differences between the groups. Statistically significant differences were found between G3 vs. G1 ($P < 0.002$), G4 (P

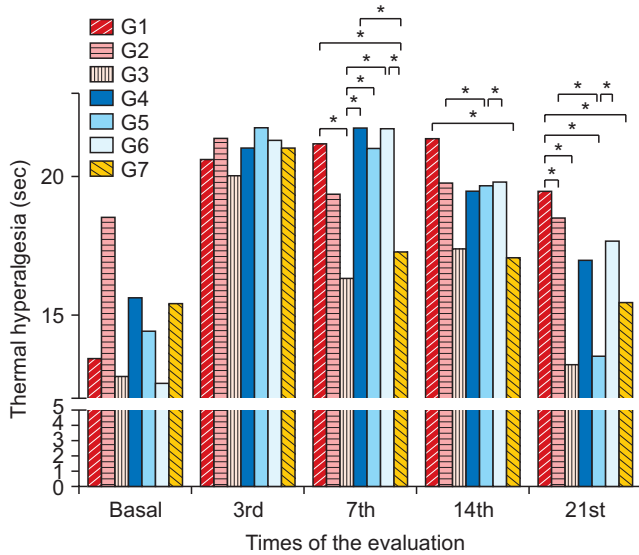


Fig. 4. Average values referring to thermal hyperalgesia between groups and evaluations. Group (G) 1: control (placebo), G2: photobiomodulation (PBM) applied to the paw with complex regional pain syndrome type I (CRPS-I) from the warm phase, G3: PBM applied to the paw with CRPS-I from the acute phase, G4: PBM applied close to the area of the region between L4 and L5 from the warm phase, G5: PBM applied close to the area of the region between L4 and L5 from the acute phase, G6: PBM applied at two points: right paw and region between L4 and L5 from the warm phase, G7: PBM applied at two points: right paw and region between L4 and L5 from the acute phase. * $P < 0.05$.

< 0.005), G5 ($P < 0.002$) and G6 ($P < 0.005$); between G7 vs. G1 ($P < 0.004$), G4 ($P < 0.009$) and G6 ($P < 0.001$) on the 7th day.

On the 14th day, significant differences were found between G1 vs. G7 ($P < 0.040$) as well as between G5 vs. G2 ($P < 0.006$) and G6 ($P < 0.002$). On the 21st day evaluation, statistically significant differences were found between G1 vs. G3 ($P < 0.015$), G5 ($P < 0.005$), G7 ($P < 0.004$); between G2 vs. G5 ($P < 0.006$) and between G6 vs. G5 ($P < 0.002$). The mean cut-off values on the 21st day were: 19.46 seconds for G1; 18.52 seconds for G2; 13.25 seconds for G3; 16.96 seconds for G4; 13.54 seconds for G5; 17.68 seconds for G6, and 15.46 seconds for G7. Only groups G3 and G5 returned to their baseline values after treatment with PBM. G1 obtained a longer cut-off time when compared to the other groups.

3. Mechanical hyperalgesia

The mean values of the mechanical hyperalgesia test (Von Frey) are shown in Fig. 5 and Table 4. No statistically significant differences were found among all the values. However, there was a pattern of withdrawal, on the 3rd and 7th day, the mean values of withdrawal were lower (0 ± 2) than on the 14th (2 ± 5) and 21st day (3 ± 6).

4. Thermography

The average values of the thermographic evaluation are found in Fig. 6 and Table 5. On the 7th day, significant differences were found between G1 vs. G4 ($P < 0.001$), G5 ($P < 0.005$), G6 ($P < 0.005$) and G7 ($P < 0.005$); between G2 and the other groups (except G1), as well as between G6 vs. G2 ($P < 0.005$), G3 ($P < 0.005$), and G4 ($P < 0.001$).

On the 14th day differences were found between G1 vs. G5 ($P < 0.001$), G6 ($P < 0.005$) and G7 ($P < 0.005$); between G2 and G3 vs. G5 ($P < 0.001$), G6 ($P < 0.005$) and G7 ($P <$

Table 3. Mean and standard deviation values for the analysis of thermal hyperalgesia according to groups and evaluations

Thermal hyperalgesia	Group						
	1	2	3	4	5	6	7
Basal	13.44 ± 5.09	18.54 ± 2.65	12.81 ± 5.27	15.62 ± 4.17	14.43 ± 4.83	12.53 ± 5.14	15.43 ± 4.05
3rd	20.61 ± 2.74	21.39 ± 1.73	20.05 ± 2.77	21.01 ± 2.23	21.78 ± 0.45	21.32 ± 1.40	21.01 ± 1.78
7th	21.17 ± 2.19	19.38 ± 3.78	16.34 ± 5.01	21.73 ± 0.49	21.02 ± 1.99	21.74 ± 0.43	17.26 ± 4.62
14th	21.36 ± 1.74	19.77 ± 3.04	17.39 ± 3.80	19.49 ± 3.99	19.70 ± 5.43	19.83 ± 2.99	17.06 ± 3.19
21st	19.47 ± 3.84	18.52 ± 4.14	13.25 ± 3.06	16.96 ± 4.18	13.55 ± 2.98	17.68 ± 3.65	15.46 ± 2.98

Group 1: control (placebo), Group 2: photobiomodulation (PBM) applied to the paw with complex regional pain syndrome type I (CRPS-I) from the warm phase, Group 3: PBM applied to the paw with CRPS-I from the acute phase, Group 4: PBM applied close to the area of the region between L4 and L5 from the warm phase, Group 5: PBM applied close to the area of the region between L4 and L5 from the acute phase, Group 6: PBM applied at two points: right paw and region between L4 and L5 from the warm phase, Group 7: PBM applied at two points: right paw and region between L4 and L5 from the acute phase, 3rd: third evaluation day, 7th: seventh evaluation day, 14th: fourteenth evaluation day, 21st: twenty-first evaluation day.

0.005); as well as between G4 vs. G6 ($P < 0.005$) and G7 ($P < 0.002$). And on the 21st day, statistical differences were found between G1 and the other groups (except G6); G2 vs. G3 ($P < 0.003$) and G6 ($P < 0.005$); between G3 vs. G2 ($P < 0.001$), G5 ($P < 0.001$) and G7 ($P < 0.005$); between G4 vs. G7 ($P < 0.001$); between G5 vs. G6 ($P < 0.006$); and between G6 vs. G7 ($P < 0.005$).

The temperature values on the seventh day of assessment were slightly higher (21.2°C-25.44°C) than at the baseline (20.22°C-24.3°C), 14th day (22.48°C-24.44°C) and 21st day (21.12°C-23.99°C).

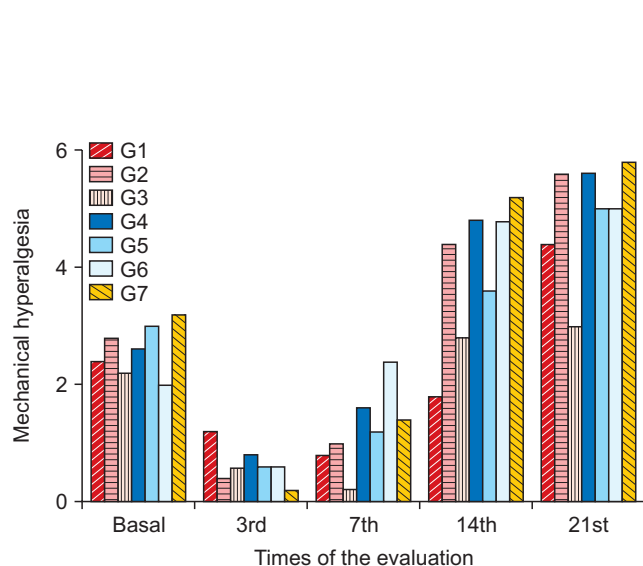


Fig. 5. Average values of the mechanical hyperalgesia test (Von Frey) between groups and evaluations. Group (G) 1: control (placebo), G2: photobiomodulation (PBM) applied to the paw with complex regional pain syndrome type I (CRPS-I) from the warm phase, G3: PBM applied to the paw with CRPS-I from the acute phase, G4: PBM applied close to the area of the region between L4 and L5 from the warm phase, G5: PBM applied close to the area of the region between L4 and L5 from the acute phase, G6: PBM applied at two points: right paw and region between L4 and L5 from the warm phase, G7: PBM applied at two points: right paw and region between L4 and L5 from the acute phase.

5. SSI and SFI

Figs. 7, 8, and Table 6 illustrate the SFI and SSI results found during the evaluations. Statistically significant differences were found between the SFI values for G1 vs. G3 ($P < 0.003$) and G7 ($P < 0.006$) on 14th day. And between G1 vs. G3 ($P < 0.003$) on the 21st day. The mean values of G1 in the 14th evaluation were -33.68 absence of unity (A.U.), G3 -14.14 A.U. and G7 -10.66 A.U., showing better results for groups G7 and G3, when compared to G1.

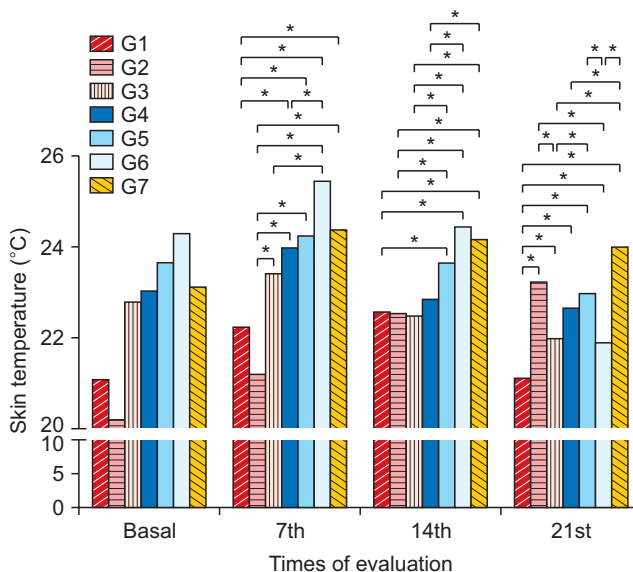


Fig. 6. Average values of the thermographic evaluation between groups and evaluations. Group (G) 1: control (placebo), G2: photobiomodulation (PBM) applied to the paw with complex regional pain syndrome type I (CRPS-I) from the warm phase, G3: PBM applied to the paw with CRPS-I from the acute phase, G4: PBM applied close to the area of the region between L4 and L5 from the warm phase, G5: PBM applied close to the area of the region between L4 and L5 from the acute phase, G6: PBM applied at two points: right paw and region between L4 and L5 from the warm phase, G7: PBM applied at two points: right paw and region between L4 and L5 from the acute phase. * $P < 0.05$.

Table 4. Mean and standard deviation values for the analysis of mechanical hyperalgesia according to groups and evaluations

Mechanical hyperalgesia	Group						
	1	2	3	4	5	6	7
Basal	2.4 ± 1.14	2.80 ± 0.84	2.20 ± 1.30	2.60 ± 1.82	3.00 ± 1.00	2.00 ± 1.58	3.20 ± 1.48
3rd	1.2 ± 0.84	0.40 ± 0.89	0.60 ± 0.55	0.80 ± 0.84	0.60 ± 0.89	0.60 ± 0.89	0.20 ± 0.45
7th	0.8 ± 1.10	1.00 ± 1.41	0.20 ± 0.45	1.60 ± 1.34	1.20 ± 1.30	2.40 ± 3.05	1.40 ± 1.52
14th	1.8 ± 2.49	4.40 ± 2.30	2.80 ± 3.11	4.80 ± 3.42	3.60 ± 2.61	4.80 ± 3.27	5.20 ± 2.05
21st	4.4 ± 3.65	5.60 ± 2.30	3.00 ± 2.12	5.60 ± 4.10	5.00 ± 1.87	5.00 ± 4.00	5.80 ± 1.48

Group 1: control (placebo), Group 2: photobiomodulation (PBM) applied to the paw with complex regional pain syndrome type I (CRPS-I) from the warm phase, Group 3: PBM applied to the paw with CRPS-I from the acute phase, Group 4: PBM applied close to the area of the region between L4 and L5 from the warm phase, Group 5: PBM applied close to the area of the region between L4 and L5 from the acute phase, Group 6: PBM applied at two points: right paw and region between L4 and L5 from the warm phase, Group 7: PBM applied at two points: right paw and region between L4 and L5 from the acute phase, 3rd: third evaluation day, 7th: seventh evaluation day, 14th: fourteenth evaluation day, 21st: twenty-first evaluation day.

Table 5. Mean and standard deviation values for thermographic according to groups and evaluations

Thermographic	Group						
	1	2	3	4	5	6	7
3rd	21.09 ± 1.74	20.23 ± 0.91	22.80 ± 0.82	23.03 ± 0.68	23.66 ± 0.39	24.30 ± 0.41	23.13 ± 1.25
7th	22.24 ± 1.92	21.20 ± 0.88	23.43 ± 0.81	23.98 ± 1.05	24.25 ± 0.63	25.45 ± 0.56	24.39 ± 1.49
14th	22.57 ± 1.25	22.54 ± 0.67	22.49 ± 1.01	22.85 ± 0.70	23.66 ± 0.86	24.45 ± 0.86	24.17 ± 0.55
21st	21.12 ± 0.50	23.22 ± 0.64	21.99 ± 0.85	22.65 ± 1.05	23.00 ± 0.69	21.89 ± 0.35	23.99 ± 0.86

Group 1: control (placebo), Group 2: photobiomodulation (PBM) applied to the paw with complex regional pain syndrome type I (CRPS-I) from the warm phase, Group 3: PBM applied to the paw with CRPS-I from the acute phase, Group 4: PBM applied close to the area of the region between L4 and L5 from the warm phase, Group 5: PBM applied close to the area of the region between L4 and L5 from the acute phase, Group 6: PBM applied at two points: right paw and region between L4 and L5 from the warm phase, Group 7: PBM applied at two points: right paw and region between L4 and L5 from the acute phase, 3rd: third evaluation day, 7th: seventh evaluation day, 14th: fourteenth evaluation day, 21st: twenty-first evaluation day.

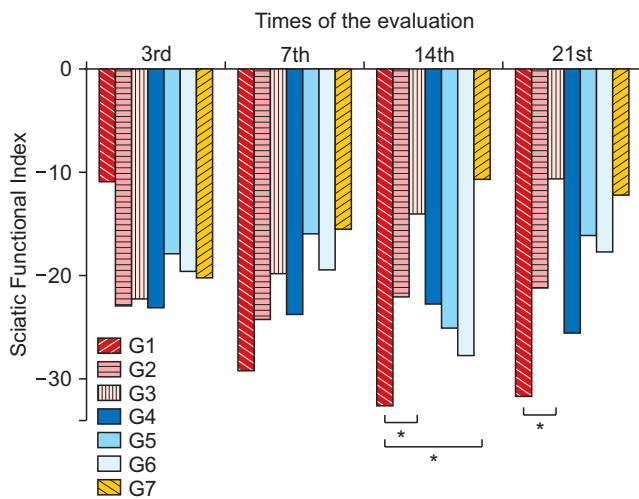


Fig. 7. Average values of Sciatic Functional Index (SFI) between groups and between evaluations. Group (G) 1: control (placebo), G2: photobiomodulation (PBM) applied to the paw with complex regional pain syndrome type I (CRPS-I) from the warm phase, G3: PBM applied to the paw with CRPS-I from the acute phase, G4: PBM applied close to the area of the region between L4 and L5 from the warm phase, G5: PBM applied close to the area of the region between L4 and L5 from the acute phase, G6: PBM applied at two points: right paw and region between L4 and L5 from the warm phase, G7: PBM applied at two points: right paw and region between L4 and L5 from the acute phase. **P* < 0.05.

Regarding the SSI values, there were significant differences only between G1 vs. G3 (*P* < 0.003) and G7 (*P* < 0.002) on the 14th day. The mean values of G1 in this evaluation were -33.15 A.U. and -10.52 A.U. for G3 and -9.70 A.U. for G7, demonstrating greater effectiveness of PBM treatment in these groups when compared to the placebo.

DISCUSSION

The CRPS-I treatment guidelines recommend a multidisciplinary approach, however, the search for an ideal treatment remains a challenge [13,34]. This is the first study to

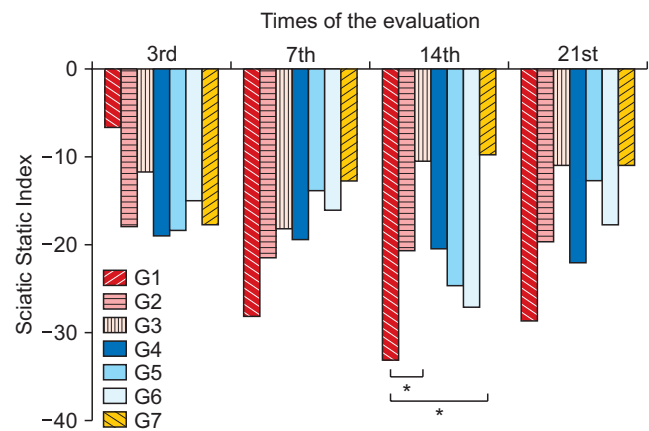


Fig. 8. Average values of Sciatic Static Index (SSI) between groups and between evaluations. Group (G) 1: control (placebo), G2: photobiomodulation (PBM) applied to the paw with complex regional pain syndrome type I (CRPS-I) from the warm phase, G3: PBM applied to the paw with CRPS-I from the acute phase, G4: PBM applied close to the area of the region between L4 and L5 from the warm phase, G5: PBM applied close to the area of the region between L4 and L5 from the acute phase, G6: PBM applied at two points: right paw and region between L4 and L5 from the warm phase, G7: PBM applied at two points: right paw and region between L4 and L5 from the acute phase. **P* < 0.05.

describe the effects of PBM with 830 nm on CRPS-I applied at different sites, the affected leg and final segment of the region between L4 and L5, and to compare the effects of PBM 830 nm introduced in the warm and acute phases of CRPS-I. Our main findings were: (1) PBM has better results when introduced in the acute phase of the CPIP model, because it effectively reduced edema and attenuated nociceptive behaviors; and (2) PBM applied directly to the affected paw showed better results than the application in the region between L4 and L5.

Some studies [13,14,24,26,32,33,39,40] have evaluated the effects of different wavelengths including 660 and 830 nm on CRPS-I, and found a reported decrease in mechanical hyperalgesia [13], decreased temperature, and early functional recovery [33] in the groups treated with PBM

Table 6. Mean and standard deviation values for the Sciatic Functional Index and Sciatic Static Index analysis according to groups and evaluations

Variable	Group						
	1	2	3	4	5	6	7
Sciatic Functional Index							
Basal	-10.90 ± 6.14	-23.00 ± 9.48	-22.31 ± 4.09	-23.21 ± 6.85	-17.97 ± 12.18	-19.60 ± 8.52	-20.24 ± 9.50
3rd	-29.22 ± 12.80	-24.25 ± 10.11	-19.86 ± 10.25	-23.86 ± 11.01	-16.03 ± 8.90	-19.52 ± 11.84	-15.57 ± 3.13
7th	-32.69 ± 9.14	-22.11 ± 9.22	-14.14 ± 5.22	-22.83 ± 8.38	-25.22 ± 8.89	-27.78 ± 9.64	-10.67 ± 7.93
14th	-31.78 ± 13.33	-21.25 ± 10.58	-10.74 ± 8.40	-25.70 ± 9.85	-16.19 ± 3.34	-17.73 ± 6.86	-12.24 ± 11.77
21st	-10.90 ± 6.14	-23.00 ± 9.48	-22.31 ± 4.09	-23.21 ± 6.85	-17.97 ± 12.18	-19.60 ± 8.52	-20.24 ± 9.50
Sciatic Static Index							
3rd	-6.65 ± 2.76	-17.95 ± 12.66	-11.73 ± 3.53	-19.06 ± 14.05	-18.35 ± 2.94	-15.04 ± 6.81	-17.77 ± 9.80
7th	-28.19 ± 17.82	-21.49 ± 14.10	-18.10 ± 8.29	-19.46 ± 11.06	-13.96 ± 8.48	-16.06 ± 12.46	-12.69 ± 5.59
14th	-33.16 ± 10.26	-20.74 ± 12.11	-10.52 ± 8.30	-20.50 ± 9.36	-24.79 ± 12.93	-27.13 ± 10.73	-9.70 ± 5.91
21st	-28.73 ± 14.38	-19.74 ± 11.93	-10.95 ± 8.61	-22.05 ± 12.60	-12.71 ± 9.09	-17.76 ± 7.08	-10.93 ± 3.94

Group 1: control (placebo), Group 2: photobiomodulation (PBM) applied to the paw with complex regional pain syndrome type I (CRPS-I) from the warm phase, Group 3: PBM applied to the paw with CRPS-I from the acute phase, Group 4: PBM applied close to the area of the region between L4 and L5 from the warm phase, Group 5: PBM applied close to the area of the region between L4 and L5 from the acute phase, Group 6: PBM applied at two points: right paw and region between L4 and L5 from the warm phase, Group 7: PBM applied at two points: right paw and region between L4 and L5 from the acute phase, 3rd: third evaluation day, 7th: seventh evaluation day, 14th: fourteenth evaluation day, 21st: twenty-first evaluation day.

830 nm. The choice of wavelength for this study was due to these results, which demonstrated greater efficacy in treating the symptoms of CRPS-I in mice. In addition, PBM 660 had shown higher attenuation (approximately 70% to 75%), while PBM 830 nm had shown approximately 60% to 68% attenuation at 1.17 and 1.66 mm thicknesses of mouse skin [24]. Previous studies also show that PBM 830 nm penetrates 54% deeper than PBM 980 nm in mouse skin [26] and has greater penetration than PBM 910 nm in spinal nerves in mice [25], demonstrating better power density distribution across tissue and providing treatment in different layers of mouse skin [26].

As previously described, CRPS-I has three stages [5]. The study by Rodrigues et al. [13] evaluated the effects of PBM 660 and 830 nm on CRPS-I and reported that mechanical hyperalgesia decreased significantly from the fourth day of application in the groups treated with PBM 660 and 830 nm, corroborating with the data of the present study, where the group treated with PBM in the acute phase (G3) obtained reduced values of mechanical hyperalgesia. These findings can be explained by the rapid action of PBM, promoting peripheral and sympathetic nerve blockade and reducing pain [17]. In addition, PBM in fluencies between 3-8 J/cm² can modulate the endogenous opioid system, reduce IL-1 β and TNF α and cause antinociceptive action [41].

In addition to the antinociceptive action, PBM reduces edema due to reduced expression of pro-inflammatory cytokines [42]. In this study, groups G3 (PBM on the paw from the acute phase) and G7 (PBM on the paw and region between L4 and L5 from the acute phase) showed better evolution in relation to edema when compared to other

groups treated from the acute phase. These findings corroborate those found by Joensen and Gjerdet [43], where PBM irradiation in the acute phase increased edema in rats after calcaneal tendon injury. A possible explanation for the increase of edema in these groups may be related to the reduction of the sensation of pain, which would increase the physical activity of these animals, promoting temporary vasodilatation and consequent edema [44].

Thus, in this study, the SFI and SSI were used to evaluate the functional quality of the subjects' gait. Our results showed that the placebo group had a lower gait quality (-27.54 ± 10.00) when compared to G3 (-16.25 ± 5.05) and G7 (-13.75 ± 4.78), both in SFI and SSI. These findings corroborate those found by Barbosa et al. [45] and Marcolino et al. [33], where they evaluated the degree of functionality inferred by SFI and SSI in experimental models treated with PBM 830 nm after sciatic nerve injury. A manuscript by Marcolino et al. [33] concluded that irradiation at 830 nm was effective in accelerating gait recovery in the first two weeks of treatment. Barbosa et al. [45] and de Souza et al. [32] concluded in their studies that PBM provided early functional recovery in the evaluated model.

Another variable evaluated in this study was the skin temperature of the limb with CRPS-I. The monitoring of a disease by means of a thermographic camera allows verification of the effectiveness of a therapeutic procedure and the progression of a disease, since there is a good correlation between temperature and the sympathetic activity of the skin [13,45]. Our findings showed several significant differences between days and groups, but the highest temperature values were found on the seventh day of evaluation. A study by Kocić et al. [14] evaluated the skin tem-

perature of individuals with CRPS-I after the application of PBM and highlighted a decrease in temperature after treatment, corroborating our findings, where the temperature was lower from the seventh day. This may happen due to the regulatory effect on skin vascular tone that PBM provides.

Although PBM has a regulatory effect on vascular tonus, the direct application in the marrow did not show good results in the treatment of CRPS-I. These findings corroborate with those found by Pires de Sousa et al. [16], where PBM doses were applied in the lumbar region (near the location of the spinal cord) and an increase in pain threshold was found after 3 hours of application, which may explain the higher values of allodynia in the groups of this study. In the study of Mandelbaum-livnat et al. [46], applications of PBM were performed in three different sites: the injured area of the peripheral nerve, segments of the spinal cord, and denervated muscle, and concluded that the treatment would be effective only by applying it directly to the injured muscle. A possible explanation is that PBM has effects mainly at the site of application, due to its interaction with the injured tissue [47].

In the research that relates CRPS-I and PBM there is no consensus on the parameters used, nor studies about relating the phases of the syndrome with the effects of PBM, which makes it difficult to compare the results and understand the mechanisms involved. Among the limitations of this study is the lack of intraclass correlation coefficient between the measures of SFI and SSI, however, it should be noted that the measures were performed by only one examiner, who had been previously trained.

The information obtained in this study allows us to report that the irradiation of PBM from the acute phase of CRPS-I was more effective than when initiated from the warm phase. And irradiation at the affected site (right paw) obtained better results when compared to irradiation at the region between L4 and L5 in reducing edema, thermal and mechanical hyperalgesia, and improving gait quality, demonstrating efficacy in treatment of CRPS-I symptoms.

ACKNOWLEDGMENTS

We are grateful to the Federal University of Santa Catarina for making the site available for this research.

CONFLICT OF INTEREST

No potential conflict of interest relevant to this article was reported.

FUNDING

No funding to declare.

ORCID

Jaqueline Betta Canever, <https://orcid.org/0000-0002-2238-0556>

Rafael Inácio Barbosa, <https://orcid.org/0000-0003-3690-3001>

Ketlyn Germann Hendler, <https://orcid.org/0000-0002-8209-1895>

Lais Mara Siqueira das Neves, <https://orcid.org/0000-0003-3862-3353>

Heloise Uliam Kuriki, <https://orcid.org/0000-0002-4610-4396>

Aderbal Silva Aguiar Júnior, <https://orcid.org/0000-0002-6825-3333>

Marisa de Cassia Registro Fonseca, <https://orcid.org/0000-0001-8187-5834>

Alexandre Márcio Marcolino, <https://orcid.org/0000-0002-2347-3797>

REFERENCES

1. De Prá SDT, Antoniazzi CTD, Ferro PR, Kudsi SQ, Campogara C, Fialho MFP, et al. Nociceptive mechanisms involved in the acute and chronic phases of a complex regional pain syndrome type 1 model in mice. *Eur J Pharmacol* 2019; 859: 172555.
2. Tajerian M, Clark JD. New concepts in complex regional pain syndrome. *Hand Clin* 2016; 32: 41-9.
3. Birklein F, O'Neill D, Schlereth T. Complex regional pain syndrome: an optimistic perspective. *Neurology* 2015; 84: 89-96.
4. Harden NR, Bruehl S, Perez RSGM, Birklein F, Marinus J, Maihofner C, et al. Validation of proposed diagnostic criteria (the "Budapest Criteria") for Complex Regional Pain Syndrome. *Pain* 2010; 150: 268-74.
5. Wei T, Guo TZ, Li WW, Kingery WS, Clark JD. Acute versus chronic phase mechanisms in a rat model of CRPS. *J Neuroinflammation* 2016; 13: 14.
6. Goh EL, Chidambaram S, Ma D. Complex regional pain syndrome: a recent update. *Burns Trauma* 2017; 5: 2.
7. Schwartzman RJ, Erwin KL, Alexander GM. The natural history of complex regional pain syndrome. *Clin J Pain* 2009; 25: 273-80.
8. Lee WH. Complex regional pain syndrome: time to study the supraspinal role? *Korean J Pain* 2015; 28: 1-3.
9. Karmarkar A, Lieberman I. Mirror box therapy for complex regional pain syndrome. *Anaesthesia* 2006; 61: 412-3.
10. Geurts JW, Smits H, Kemler MA, Brunner F, Kessels AG, van Kleef M. Spinal cord stimulation for complex regional pain syndrome type I: a prospective cohort study with long-term follow-up. *Neuromodulation* 2013; 16: 523-9.
11. Bodde MI, Dijkstra PU, den Dunnen WF, Geertzen JH. Therapy-resistant complex regional pain syndrome type I: to amputate or not? *J Bone Joint Surg Am* 2011; 93: 1799-805.

12. Krans-Schreuder HK, Bodde MI, Schrier E, Dijkstra PU, van den Dungen JA, den Dunnen WF, et al. Amputation for long-standing, therapy-resistant type-I complex regional pain syndrome. *J Bone Joint Surg Am* 2012; 94: 2263-8.
13. Rodrigues M, Cardoso RB, Kuriki HU, Marcolino AM, de Oliveira Guirro EC, Barbosa RI. Photobiomodulation decreases hyperalgesia in complex regional pain syndrome: an experimental mouse model subjected to nicotine. *Lasers Surg Med* 2020; 52: 890-6.
14. Kocić M, Lazović M, Dimitrijević I, Mančić D, Stanković A. [Evaluation of low level laser and interferential current in the therapy of complex regional pain syndrome by infrared thermographic camera]. *Vojnosanit Pregl* 2010; 67: 755-60. Serbian.
15. Smart KM, Wand BM, O'Connell NE. Physiotherapy for pain and disability in adults with complex regional pain syndrome (CRPS) types I and II. *Cochrane Database Syst Rev* 2016; 2: CD010853.
16. Pires de Sousa MV, Ferraresi C, Kawakubo M, Kaippert B, Yoshimura EM, Hamblin MR. Transcranial low-level laser therapy (810 nm) temporarily inhibits peripheral nociception: photoneuromodulation of glutamate receptors, prostatic acid phosphatase, and adenosine triphosphate. *Neurophotonics* 2016; 3: 015003.
17. de Sousa MVP, Kawakubo M, Ferraresi C, Kaippert B, Yoshimura EM, Hamblin MR. Pain management using photobiomodulation: mechanisms, location, and repeatability quantified by pain threshold and neural biomarkers in mice. *J Biophotonics* 2018; 11: e201700370.
18. Tang C, Li J, Tai WL, Yao W, Zhao B, Hong J, et al. Sex differences in complex regional pain syndrome type I (CRPS-I) in mice. *J Pain Res* 2017; 10: 1811-9.
19. Coderre TJ, Xanthos DN, Francis L, Bennett GJ. Chronic post-ischemia pain (CPIP): a novel animal model of complex regional pain syndrome-type I (CRPS-I; reflex sympathetic dystrophy) produced by prolonged hindpaw ischemia and reperfusion in the rat. *Pain* 2004; 112: 94-105.
20. Drysch M, Wallner C, Schmidt SV, Reinkemeier F, Wagner JM, Lehnhardt M, et al. An optimized low-pressure tourniquet murine hind limb ischemia reperfusion model: inducing acute ischemia reperfusion injury in C57BL/6 wild type mice. *PLoS One* 2019; 14: e0210961.
21. Gallagher JJ, Tajerian M, Guo T, Shi X, Li W, Zheng M, et al. Acute and chronic phases of complex regional pain syndrome in mice are accompanied by distinct transcriptional changes in the spinal cord. *Mol Pain* 2013; 9: 40.
22. Wei T, Li WW, Guo TZ, Zhao R, Wang L, Clark DJ, et al. Post-junctional facilitation of substance P signaling in a tibia fracture rat model of complex regional pain syndrome type I. *Pain* 2009; 144: 278-86.
23. Chen R, Yin C, Hu Q, Liu B, Tai Y, Zheng X, et al. Expression profiling of spinal cord dorsal horn in a rat model of complex regional pain syndrome type-I uncovers potential mechanisms mediating pain and neuroinflammation responses. *J Neuroinflammation* 2020; 17: 162.
24. Barbosa RI, Guirro ECO, Bachmann L, Brandino HE, Guirro RRJ. Analysis of low-level laser transmission at wavelengths 660, 830 and 904 nm in biological tissue samples. *J Photochem Photobiol B* 2020; 209: 111914.
25. Shuaib A, Bourisly AK. Photobiomodulation optimization for spinal cord injury rat phantom model. *Transl Neurosci* 2018; 9: 67-71.
26. Hudson DE, Hudson DO, Wininger JM, Richardson BD. Penetration of laser light at 808 and 980 nm in bovine tissue samples. *Photomed Laser Surg* 2013; 31: 163-8.
27. Hamblin MR, Ferraresi C, Huang YY, de Freitas LF, Carroll JD. Low-level light therapy: photobiomodulation. Bellingham, Society of Photo-Optical Instrumentation Engineers (SPIE). 2018.
28. Erthal V, Maria-Ferreira D, Werner MF, Baggio CH, Nohama P. Anti-inflammatory effect of laser acupuncture in ST36 (Zusanli) acupoint in mouse paw edema. *Lasers Med Sci* 2016; 31: 315-22.
29. Hargreaves K, Dubner R, Brown F, Flores C, Joris J. A new and sensitive method for measuring thermal nociception in cutaneous hyperalgesia. *Pain* 1988; 32: 77-88.
30. Minett MS, Eijkelkamp N, Wood JN. Significant determinants of mouse pain behaviour. *PLoS One* 2014; 9: e104458.
31. Deuis JR, Dvorakova LS, Vetter I. Methods used to evaluate pain behaviors in rodents. *Front Mol Neurosci* 2017; 10: 284.
32. de Souza LG, Marcolino AM, Kuriki HU, Gonçalves ECD, Fonseca MCR, Barbosa RI. Comparative effect of photobiomodulation associated with dexamethasone after sciatic nerve injury model. *Lasers Med Sci* 2018; 33: 1341-9.
33. Marcolino AM, Barbosa RI, das Neves LM, Mazzer N, de Jesus Guirro RR, de Cássia Registro Fonseca M. Assessment of functional recovery of sciatic nerve in rats submitted to low-level laser therapy with different fluences. An experimental study: laser in functional recovery in rats. *J Hand Microsurg* 2013; 5: 49-53.
34. de Medinaceli L, Freed WJ, Wyatt RJ. An index of the functional condition of rat sciatic nerve based on measurements made from walking tracks. *Exp Neurol* 1982; 77: 634-43.
35. Bain JR, Mackinnon SE, Hunter DA. Functional evaluation of complete sciatic, peroneal, and posterior tibial nerve lesions in the rat. *Plast Reconstr Surg* 1989; 83: 129-36.
36. Takhtfooladi MA, Jahanbakhsh F, Takhtfooladi HA, Yousefi K, Allahverdi A. Effect of low-level laser therapy (685 nm, 3 J/cm²) on functional recovery of the sciatic nerve in rats following crushing lesion. *Lasers Med Sci* 2015; 30: 1047-52.
37. Smit X, van Neck JW, Ebeli MJ, Hovius SE. Static footprint analysis: a time-saving functional evaluation of nerve repair in rats. *Scand J Plast Reconstr Surg Hand Surg* 2004; 38: 321-5.

38. National Institute of Neurological Disorders and Stroke. Complex regional pain syndrome fact sheet. Bethesda, National Institutes of Health. 2020.
39. Marcolino AM, Barbosa RI, das Neves LMS, Vinas TS, Duarte DTB, Mazzer N, et al. Low intensity laser (830 nm) functional to recover of the sciatic nerve in rats. *Acta Ortop Bras* 2010; 18: 207-11.
40. Chow RT, David MA, Armati PJ. 830 nm laser irradiation induces varicosity formation, reduces mitochondrial membrane potential and blocks fast axonal flow in small and medium diameter rat dorsal root ganglion neurons: implications for the analgesic effects of 830 nm laser. *J Peripher Nerv Syst* 2007; 12: 28-39.
41. Pereira FC, Parisi JR, Maglioni CB, Machado GB, Barragán-Iglesias P, Silva JRT, et al. Antinociceptive effects of low-level laser therapy at 3 and 8 j/cm² in a rat model of postoperative pain: possible role of endogenous opioids. *Lasers Surg Med* 2017; 49: 844-51.
42. Cotler HB, Chow RT, Hamblin MR, Carroll J. The use of low level laser therapy (LLLT) for musculoskeletal pain. *MOJ Orthop Rheumatol* 2015; 2: 00068.
43. Joensen J, Gjerdet NR, Hummelsund S, Iversen V, Lopes-Martins RA, Bjordal JM. An experimental study of low-level laser therapy in rat Achilles tendon injury. *Lasers Med Sci* 2012; 27: 103-11.
44. Bjordal JM, Couppé C, Chow RT, Tunér J, Ljunggren EA. A systematic review of low level laser therapy with location-specific doses for pain from chronic joint disorders. *Aust J Physiother* 2003; 49: 107-16.
45. Barbosa RI, Marcolino AM, de Jesus Guirro RR, Mazzer N, Barbieri CH, de Cássia Registro Fonseca M. Comparative effects of wavelengths of low-power laser in regeneration of sciatic nerve in rats following crushing lesion. *Lasers Med Sci* 2010; 25: 423-30.
46. Mandelbaum-Livnat MM, Almog M, Nissan M, Loeb E, Shapira Y, Rochkind S. Photobiomodulation triple treatment in peripheral nerve injury: nerve and muscle response. *Photomed Laser Surg* 2016; 34: 638-45.
47. Neves LMS, Gonçalves ECD, Cavalli J, Vieira G, Laurindo LR, Simões RR, et al. Photobiomodulation therapy improves acute inflammatory response in mice: the role of cannabinoid receptors/ATP-sensitive K⁺ channel/p38-MAPK signaling pathway. *Mol Neurobiol* 2018; 55: 5580-93.